

NASA Contractor Report 4570

1N-34
209769
29P

On Prediction of Equilibrium States in Homogeneous Compressible Turbulence

Ridha Abid

(NASA-CR-4570) ON PREDICTION OF
EQUILIBRIUM STATES IN HOMOGENEOUS
COMPRESSIBLE TURBULENCE (High
Technology Corp.) 29 p

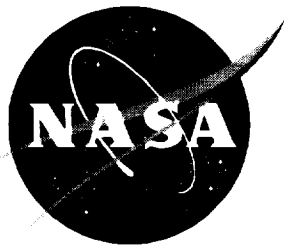
N94-26467

Unclass

H1/34 0209769

Contract NAS1-19299
Prepared for Langley Research Center

March 1994



On Prediction of Equilibrium States in Homogeneous Compressible Turbulence

Ridha Abid

High Technology Corporation • Hampton, Virginia

ON PREDICTION OF EQUILIBRIUM STATES IN HOMOGENEOUS COMPRESSIBLE TURBULENCE

Ridha Abid

High Technology Corporation
NASA Langley Research Center
Hampton, VA 23681

ABSTRACT

Direct numerical simulations of compressible, homogeneous, turbulent shear flows are used to evaluate Reynolds stress models. Three pressure-strain models, which are either linear, quadratic, or cubic in the anisotropy tensor, are considered. Dilatational dissipation and pressure-dilatation models are inserted into the Reynolds stress closure. Results show that variable-density extensions of incompressible pressure-strain correlation models do not correctly capture the compressibility effects seen in the direct simulations. In particular, the increase in the anisotropy of normal stresses and the reduction in the shear stress are not reproduced by any of the models. Also, the use of the incompressible form of the dissipation-rate equation to determine the solenoidal part of the dissipation is found to be questionable.

1. INTRODUCTION

A resurgence of interest in hypersonics has emerged, which is driven by advanced new applications such as high-speed civil transport aircraft, supersonic combustion ramjets and transatmospheric vehicles. These new applications bring into prominence some critical items that have limited the effectiveness of computational fluid dynamics codes used as tools for hypersonic system design. Chief among these is compressible turbulence modeling. Several turbulence models of varying degrees of complexity have been developed that range from the simplest algebraic or zero-equation model to the full Reynolds stress closure. Most of these models are simple extensions of their incompressible counterparts, where compressibility effects are incorporated into the models through changes in the mean density. However, many studies have shown that this type of model is unable to reproduce some features of flows that depend on compressibility, such as the reduction in the spreading rate of the compressible mixing layer as the Mach number increases. Thus, a better understanding of the effects of compressibility on flow turbulence is needed to improve current turbulence models.

Recently, direct numerical simulation (DNS) of compressible, homogeneous turbulent shear flow by Blaisdell (1990) has shown that the growth of turbulent kinetic energy decreases as the Mach number increases. The reduction is due to two compressibility terms: the dilatational dissipation and pressure-dilatation correlation, which explicitly appear in the turbulent kinetic energy and mean temperature equations. Zeman (1990, 1991) and Sarkar (1991, 1992) have modeled the additional terms; the inclusion of the two terms in two-equation turbulence models leads to a significant improvement in predicting the reduction in spreading rate with increasing Mach number.

In this paper, an assessment of Reynolds stress models in predicting compressible homogeneous shear flow is conducted with the DNS of Blaisdell (1990). Three pressure-strain correlation models, which are variable-density extensions of their incompressible counterparts, are considered. These models are either linear, quadratic, or cubic in the anisotropy stress tensor. The dilatational dissipation and pressure-dilatation correlation, which are the only explicit compressibility terms, are inserted into the Reynolds stress closure. Particular attention will be paid to the ability of each turbulence model to predict equilibrium states accurately.

2. MATHEMATICAL FORMULATION

In compressible, turbulent flows, two averaging techniques are commonly used to define the mean and fluctuating parts of a turbulent variable. Usually, conventional Reynolds

averages are used for the pressure p and the density ρ ; Favre averages are used for the velocity u_i and the temperature T . Thus, any dependent variable f can be decomposed into mean and fluctuating parts in two ways:

$$f = \bar{f} + f', \quad f = \tilde{f} + f'' \quad (1)$$

where the overbar represents the Reynolds average, the tilde denotes the Favre average, and the primes and double primes are, respectively, the deviations from the Reynolds average and the mass-weighted average. The Favre average \tilde{f} is a density-weighted Reynolds average

$$\tilde{f} = \frac{\overline{\rho f}}{\bar{\rho}} \quad (2)$$

We will consider the problem of compressible, homogeneous shear flow. In this problem, an initially decaying, compressible turbulence is subjected to a uniform shear S with the corresponding mean velocity gradients

$$\tilde{u}_{i,j} = S\delta_{1,i}\delta_{2,j} \quad (3)$$

The flow is assumed to be an ideal gas, which satisfies the equation of state $\bar{p} = \bar{\rho}R\tilde{T}$. The evolution equation of the mean temperature, derived from the energy equation, is given by

$$c_v \frac{D\tilde{T}}{Dt} = \varepsilon - \pi_d \quad (4)$$

where ε is the total dissipation rate, $\pi_d = \overline{p'd'}/\bar{p}$ is the specific pressure-dilatation, and c_v is the specific heat at constant volume.

For a compressible homogeneous shear flow at high Reynolds numbers, the Favre-averaged Reynolds stress tensor $\tau_{ij} = \overline{u_i''u_j''}$ is a solution of the transport equation

$$\frac{D\tau_{ij}}{Dt} = P_{ij} + \Pi_{ij} - \frac{2}{3}\varepsilon\delta_{ij} + \frac{2}{3}\pi_d\delta_{ij} \quad (5)$$

where Π_{ij} is the deviatoric part of the pressure-strain correlation and $P_{ij} = -\tau_{ik}\tilde{u}_{j,k} - \tau_{jk}\tilde{u}_{i,k}$ is the production term. Here, the Kolmogorov hypothesis of isotropy is invoked to model the dissipation rate tensor.

The transport equation for the turbulent kinetic energy $K = \overline{u_i''u_i''}/2$ is obtained by contracting indices in Eq. (5) as

$$\frac{DK}{Dt} = \mathcal{P} - \varepsilon + \pi_d \quad (6)$$

where $\mathcal{P} = -\tau_{ij}\tilde{u}_{ij}$ is the turbulence production.

As shown by Zeman and Sarkar, the dissipation rate of compressible homogeneous flow at high Reynolds numbers can be decomposed into a solenoidal or incompressible part, ε_s , and a compressible part, ε_d as

$$\varepsilon = \varepsilon_s + \varepsilon_d \quad (7)$$

where $\varepsilon_s = \overline{\nu \omega'_i \omega'_i}$ and $\varepsilon_d = \frac{2}{3} \overline{\nu (u'_{i,i})^2}$ given that ν is the kinematic viscosity and ω'_i is the fluctuating vorticity. Direct simulations of compressible, homogeneous shear flows show that ε_s is largely independent of compressibility and that the growth of turbulent kinetic energy decreases as the Mach number increases because of the augmented contribution of the compressible dissipation. Therefore, ε_d is modeled and ε_s is obtained by solving the incompressible form of the dissipation equation

$$\frac{D\varepsilon_s}{Dt} = -C_{\varepsilon 1} \frac{\varepsilon_s}{K} \tau_{ij} \tilde{u}_{i,j} - C_{\varepsilon 2} \frac{\varepsilon_s^2}{K} \quad (8)$$

where $C_{\varepsilon 1}$ and $C_{\varepsilon 2}$ are closure coefficients that are model dependent. The models of the dilatational dissipation and pressure-dilatation correlation considered are

Sarkar

$$\varepsilon_c = 0.5 M_t^2 \varepsilon_s \quad (9)$$

$$\overline{p'd'} = -0.15 \bar{p} \mathcal{P} M_t + 0.2 \bar{p} \varepsilon_s M_t^2 \quad (10)$$

where $M_t = \sqrt{2K/\gamma R \tilde{T}}$ is the turbulent Mach number and γ is the ratio of specific heats (= 1.4).

Zeman

$$\varepsilon_c = 0.75(1 - \exp(-((M_t - 0.1)/0.6)^2)) \varepsilon_s \quad (11)$$

$$\overline{p'd'} = (\bar{p}\gamma)^{-1} \left(\frac{\bar{p}^2 - p_e^2}{\tau_f} \right) = -0.5 \frac{D}{Dt} \left(\frac{\bar{p}^2}{\gamma \bar{p}} \right) \quad (12)$$

with

$$\tau_f = 0.4 \frac{K}{\varepsilon_s} M_t \quad (13)$$

$$\bar{p}_e^2 = 2 \bar{p}^2 K \gamma R \tilde{T} \left(\frac{M_t^2 + M_t^4}{1 + M_t^2 + M_t^4} \right) \quad (14)$$

Finally, we consider incompressible pressure-strain models, which are modeled as linear functions of the mean velocity gradients with coefficients that depend algebraically on the anisotropy tensor and the turbulent dissipation rate. Compressibility effects are incorporated through changes in density. Three models will be analyzed: the Launder, Reece, and Rodi (*LRR*) model (1975); the Fu, Launder, and Tselepidakis (*FLT*) model (1987); and the

Speziale, Sarkar, and Gatski (*SSG*) model (1991). These models are either linear (*LRR*), quadratic (*SSG*), or cubic (*FLT*) in the anisotropy tensor

$$b_{ij} = \frac{1}{2K}(\tau_{ij} - \frac{2}{3}K\delta_{ij}) \quad (15)$$

and are assumed to be only functions of the anisotropy \mathbf{b} and the symmetric and antisymmetric parts of the mean velocity gradient

$$\tilde{S}_{ij} = \frac{1}{2} \left(\frac{\partial \tilde{u}_i}{\partial x_j} + \frac{\partial \tilde{u}_j}{\partial x_i} \right) \quad (16a)$$

$$\tilde{W}_{ij} = \frac{1}{2} \left(\frac{\partial \tilde{u}_i}{\partial x_j} - \frac{\partial \tilde{u}_j}{\partial x_i} \right) \quad (16b)$$

The high Reynolds number forms of these models are

Launder, Reece, and Rodi (LRR)

$$\begin{aligned} \Pi_{ij}(\mathbf{b}, \tilde{\mathbf{S}}, \tilde{\mathbf{W}}) = & -C_1 \varepsilon b_{ij} + C_2 K (\tilde{S}_{ij} - \frac{1}{3} \tilde{S}_{kk} \delta_{ij}) + C_3 K (b_{ik} \tilde{S}_{jk} + b_{jk} \tilde{S}_{ik} - \frac{2}{3} b_{kl} \tilde{S}_{kl} \delta_{ij}) \\ & + C_4 K (b_{ik} \tilde{W}_{jk} + b_{jk} \tilde{W}_{ik}) \end{aligned} \quad (17a)$$

where

$$\begin{aligned} C_1 &= 3, \quad C_2 = 0.8, \\ C_3 &= 1.745, \quad C_4 = 1.309 \end{aligned} \quad (17b)$$

Fu, Launder, and Tselepidakis (FLT)

$$\begin{aligned} \Pi_{ij}(\mathbf{b}, \tilde{\mathbf{S}}, \tilde{\mathbf{W}}) = & 120II\sqrt{F}\varepsilon \left[b_{ij} + \frac{6}{5} \left(b_{ik} b_{kj} - \frac{1}{3} b_{kl} b_{kl} \delta_{ij} \right) \right] \\ & + \frac{4}{5} K (\tilde{S}_{ij} - \frac{1}{3} \tilde{S}_{kk}) + \frac{6}{5} K \left(b_{ik} \tilde{S}_{jk} + b_{jk} \tilde{S}_{ik} - \frac{2}{3} b_{kl} \tilde{S}_{kl} \delta_{ij} \right) \\ & + \frac{26}{15} K (b_{ik} \tilde{W}_{jk} + b_{jk} \tilde{W}_{ik}) \\ & + \frac{4}{5} K \left[(b_{ik} b_{kl} \tilde{S}_{jl} + b_{jk} b_{kl} \tilde{S}_{il} - 2b_{ik} \tilde{S}_{kl} b_{lj} - 3b_{kl} \tilde{S}_{kl} b_{ij}) \right. \\ & \quad \left. + (b_{ik} b_{kl} \tilde{W}_{jl} + b_{jk} b_{kl} \tilde{W}_{il}) \right] \\ & - 4rK \left[8II(b_{ik} \tilde{W}_{jk} + b_{jk} \tilde{W}_{ik}) + 12(b_{ik} b_{kl} \tilde{W}_{lm} b_{mj} + b_{jk} b_{kl} \tilde{W}_{lm} b_{mi}) \right] \end{aligned} \quad (18a)$$

where

$$\begin{aligned} II &= -\frac{1}{2}b_{ij}b_{ij}, \quad III = \frac{1}{3}b_{ij}b_{jk}b_{kl} \\ r &= 0.7, \quad F = 1 + 9II + 27III \end{aligned} \quad (18b)$$

Speziale, Sarkar, and Gatski (SSG)

$$\begin{aligned} \Pi_{ij}(\mathbf{b}, \tilde{\mathbf{S}}, \tilde{\mathbf{W}} &= -(C_1\varepsilon + C_1^*\mathcal{P})b_{ij} + C_2\varepsilon \left(b_{ik}b_{kj} - \frac{1}{3}b_{kl}b_{kl}\delta_{ij} \right) \\ &+ \left(C_3 - C_3^*\sqrt{b_{ij}b_{ij}} \right) K \left(\tilde{S}_{ij} - \frac{1}{3}\tilde{S}_{kk} \right) \\ &+ C_4K \left(b_{ik}\tilde{S}_{jk} + b_{jk}\tilde{S}_{ik} - \frac{2}{3}b_{kl}\tilde{S}_{kl}\delta_{ij} \right) \\ &+ C_5K(b_{ik}\tilde{W}_{jk} + b_{jk}\tilde{W}_{ik}) \end{aligned} \quad (19a)$$

where $\mathcal{P} = -\tau_{kl}\tilde{S}_{kl}$ is the turbulence production and

$$\begin{aligned} C_1 &= 3.4, \quad C_1^* = 1.80, \quad C_2 = 4.2, \\ C_3 &= 0.8, \quad C_3^* = 1.30, \quad C_4 = 1.25, \\ C_5 &= 0.40 \end{aligned} \quad (19b)$$

As mentioned previously, the closure coefficients $C_{\varepsilon 1}$, $C_{\varepsilon 2}$, and C_ε for the turbulent dissipation rate equation (Eq. (8)) are model dependent. The values for these coefficients are given by

Launder, Reece, and Rodi (LRR)

$$C_{\varepsilon 1} = 1.44, \quad C_{\varepsilon 2} = 1.90 \quad (20a)$$

Fu, Launder, and Tselepidakis (FLT)

$$C_{\varepsilon 1} = 1.45, \quad C_{\varepsilon 2} = 1.90 \quad (20b)$$

Speziale, Sarkar, and Gatski (SSG)

$$C_{\varepsilon 1} = 1.44, \quad C_{\varepsilon 2} = 1.83 \quad (20c)$$

In the *LRR* and *SSG* models, the dissipation rate ε_{ij} is modeled through the usual isotropic assumption $\varepsilon_{ij} = \frac{2}{3}\varepsilon\delta_{ij}$, whereas in the *FLT* model the tensor dissipation rate explicitly accounts for anisotropic effects:

$$\varepsilon_{ij} = \frac{2}{3}\varepsilon\sqrt{F}\delta_{ij} + 2(1 - \sqrt{F})\varepsilon b_{ij} \quad (21)$$

where F has been defined previously in Eq. (18b).

Calculations of compressible, homogeneous shear flows show that the Reynolds stresses, the dissipation rate, and the mean temperature grow exponentially, so that the anisotropy tensor b_{ij} , the shear parameter SK/ε_s and the turbulent Mach number M_t achieve equilibrium values that are independent of the initial conditions. Therefore, the system of equations for τ_{ij} , ε , and \tilde{T} is nondimensionalized and is recast into an equivalent set of equations for ε_s/SK , b_{ij} , K , and M_t as follows:

$$\frac{DK^*}{Dt^*} = -(2b_{12} + (\frac{\varepsilon - \pi_d}{SK}))K^* \quad (16)$$

$$\frac{DM_t^2}{Dt^*} = M_t^2(\frac{\varepsilon_s}{SK})(\frac{\mathcal{P}}{\varepsilon_s} - (\frac{\varepsilon - \pi_d}{\varepsilon_s})(1 + \sigma M_t^2)) \quad (17)$$

$$\frac{D}{Dt^*}(\frac{\varepsilon_s}{SK}) = (\frac{\varepsilon_s}{SK})^2((C_{\varepsilon 1} - 1)(\frac{\mathcal{P}}{\varepsilon_s} - (C_{\varepsilon 2} - (\frac{\varepsilon - \pi_d}{\varepsilon_s}))) \quad (18)$$

$$\frac{Db_{ij}}{Dt^*} = \frac{\Pi_{ij}}{2SK} + (\frac{P_{ij}}{\varepsilon_s} - \frac{2\mathcal{P}}{3\varepsilon_s}\delta_{ij})(\frac{\varepsilon_s}{2SK}) - (\frac{\mathcal{P}}{\varepsilon_s} - \frac{\varepsilon}{\varepsilon_s} + \frac{\pi_d}{\varepsilon_s})(\frac{\varepsilon_s}{SK})b_{ij} \quad (19)$$

where $t^* = St$ is the dimensionless time, $K^* = K/K_0$, K_0 is the initial value of turbulent kinetic energy, and $\sigma = \gamma(\gamma - 1)/2$. An additional equation, Eq. (12), is needed when Zeman's model is used.

This system of nonlinear ordinary differential equations associated with each Reynolds stress model is solved subject to the initial conditions

$$K^* = 1, \quad \frac{\varepsilon_s}{SK} = 0.45, \quad M_t^2 = 0.094,$$

$$b_{11} = 0.124, \quad b_{22} = -0.106, \quad b_{12} = -0.187$$

at time $t^* = 0$, which is taken from the DNS of Blaisdell (run Sha192) at $t^* = 2$. The reason for this is that the initial conditions of the DNS at $t^* = 0$ are nonphysical. See Speziale et al. (1992). The system was integrated with a fourth-order Runge-Kutta scheme. The equilibrium states for each turbulence model are obtained numerically. A comparison of the predictions of the models with the DNS data will be made in the next section.

4. RESULTS AND DISCUSSION

The predictions of the SSG, LRR, and FLT models with Sarkar's compressibility corrections will be compared with the DNS results of Blaisdell (run Sha192).

Figures 1 and 2 show the time evolution of the turbulent kinetic energy and the turbulent Mach number, predicted by the SSG model for two initial turbulent Mach numbers $M_{t0} = 0$ and $M_{t0} = 0.307$. These figures clearly show that a variable-density extension of the SSG model is not capable of capturing the decrease of the growth rate of turbulent kinetic energy as the turbulent Mach number increases. Explicit compressibility corrections are needed to predict the trends of the DNS. However, the model SSG overpredicts the growth rate of solenoidal and total dissipation (Figs. 3 and 4), which accounts for the overly large equilibrium value of the shear parameter (Fig. 5). Also, the differences in the predictions between turbulence models are shown (Figs. 6 - 10). The SSG and FLT models reproduce the results fairly well. However, the LRR model performs poorly because it was not well calibrated in incompressible, homogeneous shear flow. See Abid and Speziale (1993).

In Figures 11 - 13, the model predictions for the time evolution of Reynolds stress anisotropies are shown. All of the models substantially underpredict the Reynolds stress anisotropies in comparison with the results of the DNS. Also, the relaxation of b_{ij} to their equilibrium states has not been captured by all the models. As pointed out by Speziale, Gatski, and Sarkar (1992), the long time behavior of turbulence models is tied to their ability to predict the equilibrium values.

In fact, all the models predict exponential long time behavior, i.e., K , ε , \tilde{T} , and τ_{ij} proportional to $\exp(\lambda_\infty t^*)$, where λ_∞ is the equilibrium growth rate given by

$$\lambda_\infty = -2(b_{12})_\infty - \left(\frac{\varepsilon - \pi_d}{SK}\right)_\infty \quad (20)$$

The equilibrium states obtained from the various turbulence models are compared with the DNS data of Rogers et al. (1986) for incompressible homogeneous shear flow (table I) and the DNS data of Blaisdell (1990) for compressible homogeneous shear flow with Sarkar's model (table II). Several observations in regard to these results are noteworthy: the Reynolds stress anisotropies $(b_{ij})_\infty$ and the shear parameter $(SK/\varepsilon_s)_\infty$ are underpredicted by all models, particularly $(b_{11})_\infty$; the shear stress $(b_{12})_\infty$ is erroneously predicted to be insensitive to the compressibility effects; and the SSG and LRR models predict the observed trend that $(b_{11})_\infty$ increases as a function of the turbulent Mach number M_t (however the FLT model erroneously predicts the opposite trend of the DNS data). Similar conclusions are drawn when Zeman's model is used. See table III.

All of the turbulence models are clearly incapable of properly accounting for the effects of compressibility on turbulent shear flow. The failure of the Reynolds stresses to predict

the increase in the anisotropy of normal stresses and the reduction in the shear stress is partly due to the use of the incompressible pressure-strain correlation models. As shown by Blaisdell and Sarkar (1993), the contribution of the compressibility to the pressure-strain correlation is large and must be taken into account.

Another deficiency of the turbulence models considered in this study lies in the use of the incompressible form of the dissipation equation to obtain the solenoidal part of the dissipation rate. The results presented in tables I and II show clearly that $(\mathcal{P}/\varepsilon_s)_\infty$ is erroneously predicted to be sensitive to the compressibility effects. When an equilibrium state is achieved, Eq. (18) gives

$$\left(\frac{\mathcal{P}}{\varepsilon_s}\right)_\infty = \frac{C_{\varepsilon 2} - 1}{C_{\varepsilon 1} - 1} - \left(\frac{1}{C_{\varepsilon 1} - 1}\right)\left(\frac{\varepsilon_d - \pi_d}{\varepsilon_s}\right) \quad (21)$$

where the first term in the right side represents the equilibrium value of $\mathcal{P}/\varepsilon_s$ in incompressible, homogeneous shear flow. Equation (21) clearly shows that the erroneous prediction of $(\mathcal{P}/\varepsilon_s)_\infty$ is directly tied to the solenoidal dissipation equation. This conclusion can be reached in other ways.

The value of $(\mathcal{P}/\varepsilon_s)_\infty$ can be determined from Eq. (17) as

$$\left(\frac{\mathcal{P}}{\varepsilon_s}\right)_\infty = \left(1 + \left(\frac{\varepsilon_d - \pi_d}{\varepsilon_s}\right)\right)(1 + \sigma M_{t\infty}^2) \quad (22)$$

The combination of Eqs. (21) and (22) leads to

$$\left(\frac{\mathcal{P}}{\varepsilon_s}\right)_\infty = \frac{C_{\varepsilon 2}}{(C_{\varepsilon 1} - 1 + \frac{1}{1 + \sigma M_{t\infty}^2})} \quad (23)$$

The above equation, which is independent of the dilatational dissipation and pressure-dilatation models, shows that $(\mathcal{P}/\varepsilon_s)_\infty$ cannot be insensitive to the compressibility effects as seen in the direct simulations, otherwise Eq. (23) will predict nonphysical values for M_t ($M_{t\infty} = 1.7$ when $(\mathcal{P}/\varepsilon_s)_\infty = 1.84$). Note that the system of Eqs. (16)-(19) will predict nonphysical results for $M_{t\infty}$ if the explicit compressibility equations are not included.

4. CONCLUDING REMARKS

Three Reynolds stress models have been evaluated for the problem of compressible, homogeneous shear flow. The dilatational dissipation and pressure-dilatation correlation models, formulated by Zeman and Sarkar, have been inserted in the Reynolds stress closure. Comparisons between the predictions of the various models and the direct numerical simulation of Blaisdell have been made.

All three Reynolds stress models fail to capture the compressibility effects seen in the direct simulations. In particular, the increase in anisotropy of the normal stresses and the

reduction in the shear stress are not reproduced by any of the models. This result is partly due to the use of variable density extensions of incompressible pressure-strain models. Thus, dilatational effects on the pressure-strain correlation must be identified and accounted for in compressible turbulence modeling.

An analysis of the predictions of the equilibrium states has shown that use of the incompressible form of the dissipation to determine the solenoidal dissipation rate is another source of inaccuracy in the predictions. In particular, the erroneous prediction of $(\mathcal{P}/\varepsilon_s)_\infty$ is directly tied to the solenoidal dissipation equation.

The present study indicates the need for further direct numerical simulations of compressible, homogeneous shear flows. Such simulations could be used to distinguish between compressibility and low Reynolds number effects and to provide more information on the equilibrium states.

REFERENCES

- Abid, R. and Speziale, C. G., 1993, "Predicting equilibrium states with Reynolds stress closures in channel flow and homogeneous shear flow," *Phys. Fluids A* **5**, pp. 1151-1158.
- Blaisdell, G. A., 1990, "Numerical simulations of compressible homogeneous turbulence," *Ph.D. Thesis*, Mechanical Engineering Dept., Stanford University, Stanford, California.
- Blaisdell, G. A. and Sarkar, S., 1993, "Investigation of the pressure strain correlation in compressible homogeneous turbulent shear flow," in *FED* **151**, Transitional and Turbulent Compressible Flows.
- Fu, S., Launder, B. E. and Tselepedikas, D. P., 1987, "Accommodating the effect of high strain rates in modeling the pressure-strain correlation," UMIST Mechanical Engineering Department Report TFD/87/5.
- Launder, B. E., Reece, G. and Rodi, W., 1975, "Progress in the development of a Reynolds stress turbulence closure," *J. Fluid Mech.* **68**, p. 637.
- Rogers, M. M., Moin, P. and Reynolds, W. C., 1986, "The structure and modeling of the hydrodynamic and passive scalar fields in homogeneous turbulent shear flows," *Technical Report* TF-25, Stanford university, Stanford, California.
- Sarkar, S., Erlebacher, G. and Hussaini, M. Y., 1991, "Direct simulations of compressible turbulence in a shear flow," *Theoret. Comput. Fluid Dynamics* **2**, pp. 291-305.
- Sarkar, S., 1992, "The pressure-dilatation correlation in compressible flows," *Phys. Fluids A* **4**, pp. 1251-1258.
- Speziale, C. G., Sarkar, S. and Gatski, T. B., 1991, "Modeling the pressure-strain correlation of turbulence: An invariant dynamical systems approach," *J. Fluid Mech.* **227**, p. 245.
- Speziale, G. S., Gatski, T. B. and Sarkar, S., 1992, "On testing models for the pressure-strain correlation of turbulence using direct simulations," *Phys. Fluids A* **4**, pp. 2887-2899.
- Zeman, O., 1990, "Dilatation dissipation: The concept and application in modeling compressible mixing layers," *Phys. Fluids A* **2**, p. 178.
- Zeman, O. and Blaisdell, G.A., 1991, "New physics and models for compressible turbulent flows," in *Advances in Turbulence 3*, A. V. Johanson and P. H. Alfredson eds., Springer Verlag, Berlin, pp. 445-454.

Equilibrium Values	LRR Model	SSG Model	FLT Model	DNS Data
b_{11}	0.155	0.219	0.208	0.215
b_{12}	-0.187	-0.164	-0.146	-0.158
b_{22}	-0.121	-0.146	-0.144	-0.153
b_{33}	-0.004	-0.073	-0.064	-0.062
SK/ε_s	5.34	5.77	6.84	5.70
P/ε_s	2.0	1.88	2.0	1.80

Table 1. Predicted Equilibrium Values for Incompressible Homogeneous Shear Flow.

Equilibrium Values	LRR Model	SSG Model	FLT Model	DNS Data
b_{11}	0.166	0.230	0.189	0.424
b_{12}	-0.187	-0.165	-0.148	-0.118
b_{22}	-0.130	-0.148	-0.138	-0.236
b_{33}	-0.036	-0.082	-0.051	-0.188
SK/ε_s	3.77	4.11	4.77	7.82
M_t	0.65	0.60	0.65	0.51
P/ε_s	1.41	1.36	1.41	1.84

Table 2. Predicted Equilibrium Values for Compressible Homogeneous Shear Flow with Sarkar's Model.

Equilibrium Values	LRR Model	SSG Model	FLT Model	DNS Data
b_{11}	0.167	0.231	0.187	0.424
b_{12}	-0.191	-0.167	-0.148	-0.118
b_{22}	-0.131	-0.148	-0.137	-0.236
b_{33}	-0.036	-0.083	-0.050	-0.188
SK/ε_s	3.59	3.95	4.61	7.82
M_t	0.48	0.45	0.48	0.51
P/ε_s	1.41	1.36	1.41	1.84

Table 3. Predicted Equilibrium Values for Compressible Homogeneous Shear Flow with Zeman's Model.

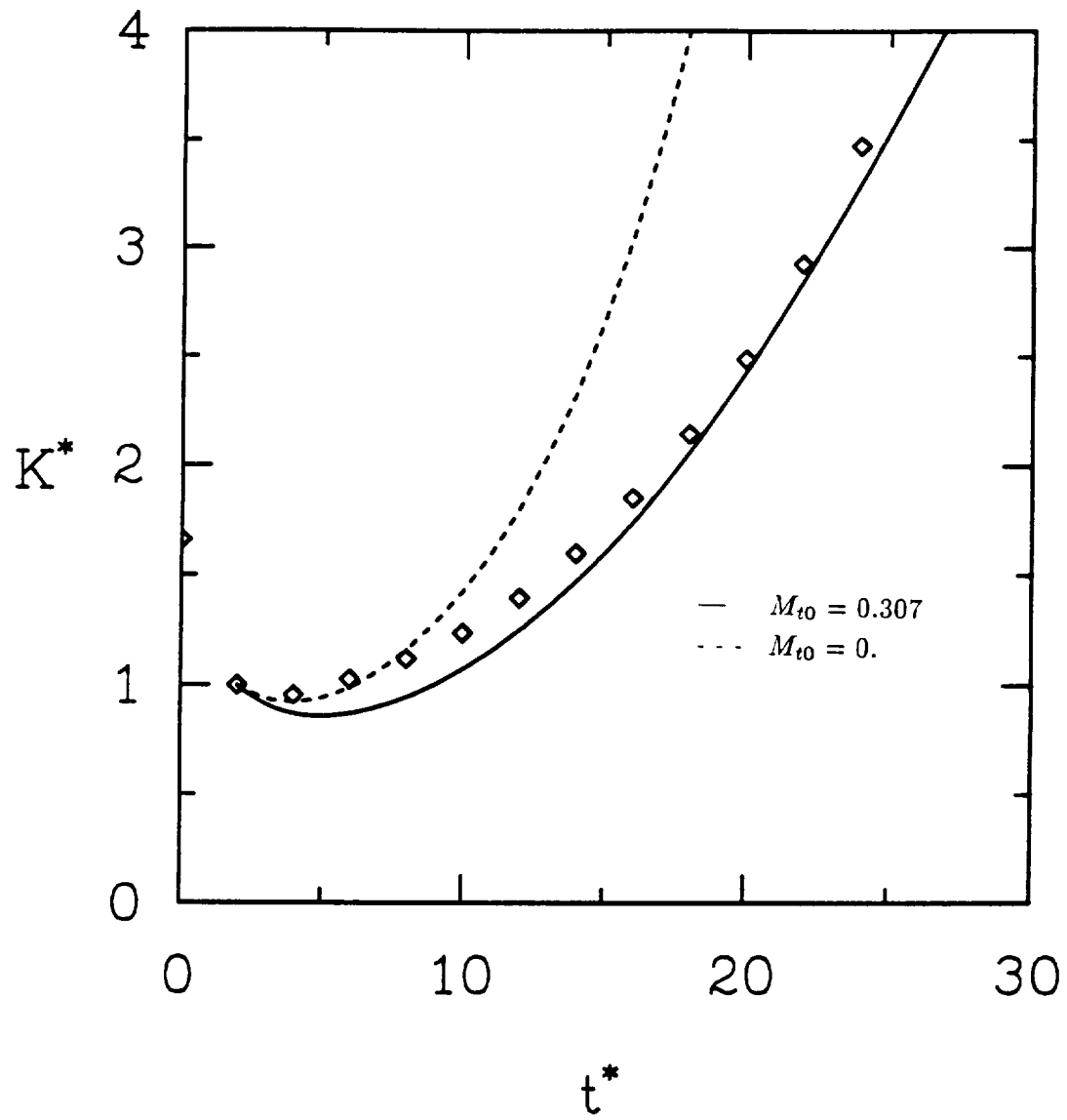


Figure 1. Comparison of the predictions of the SSG model for the time evolution of the turbulent kinetic energy with the DNS results of Blaisdell.

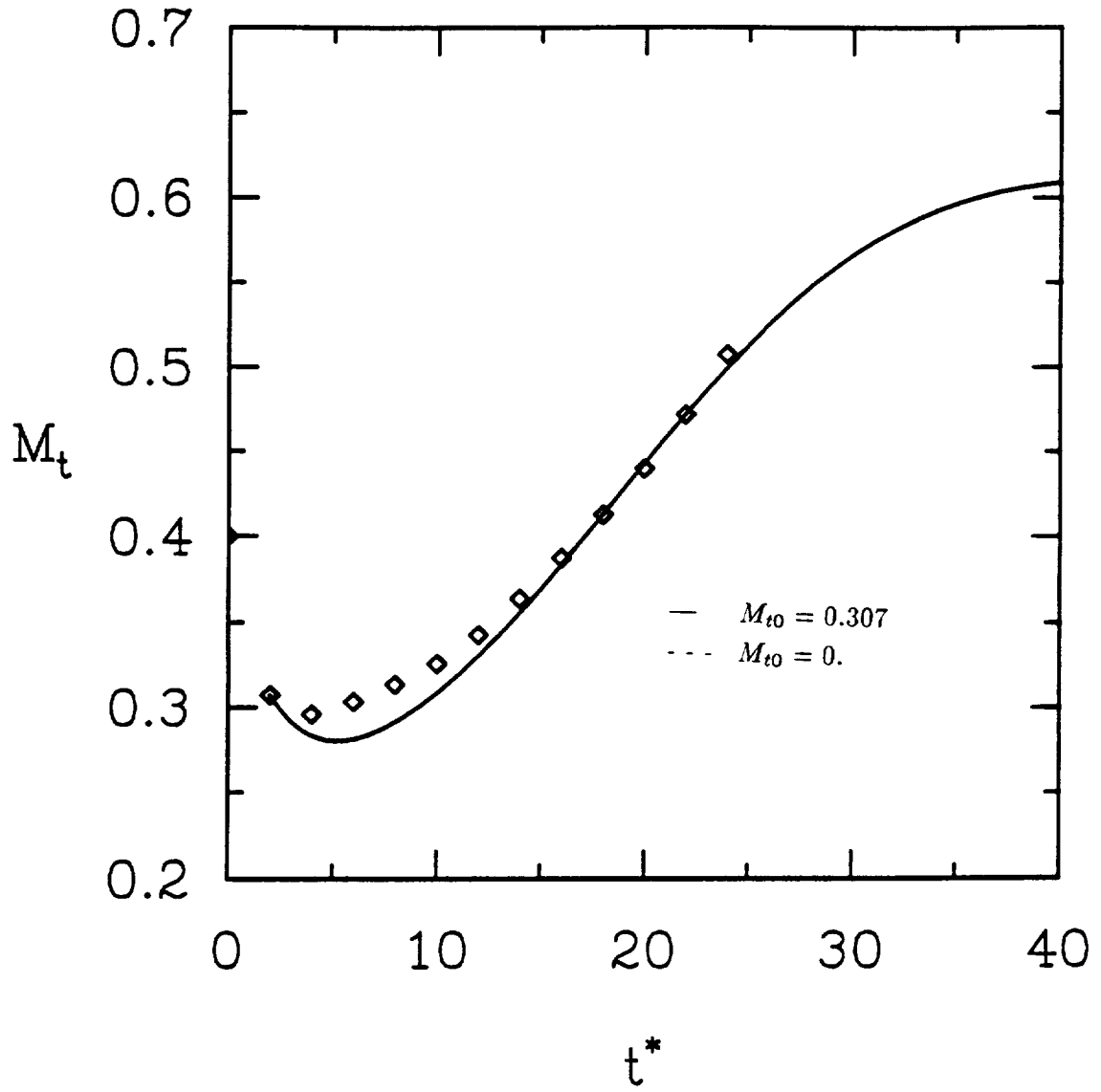


Figure 2. Comparison of the predictions of the SSG model for the time evolution of the turbulent Mach number with the DNS results of Blaisdell.

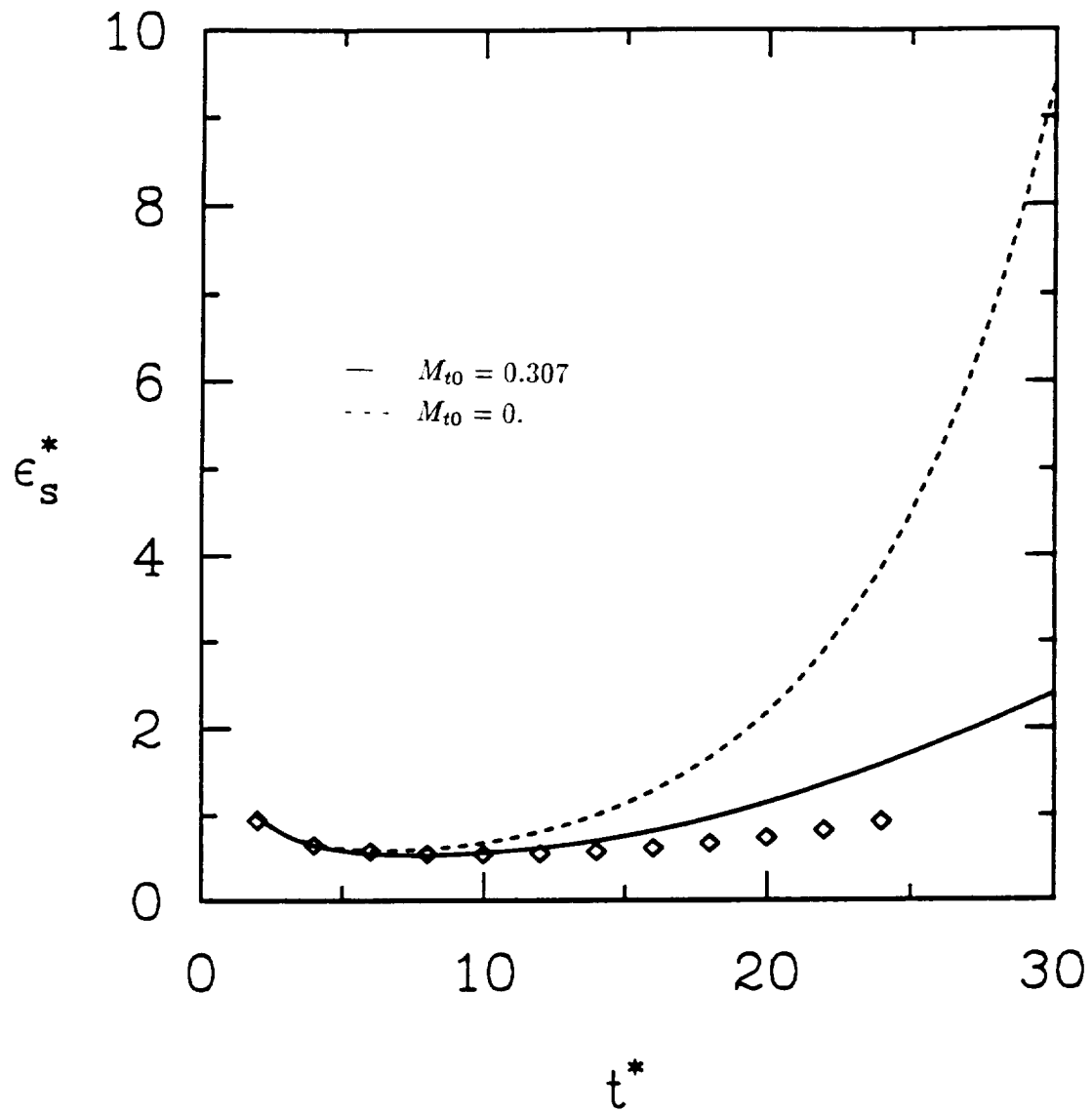


Figure 3. Comparison of the predictions of the SSG model for the time evolution of the solenoidal dissipation-rate with the DNS results of Blaisdell.

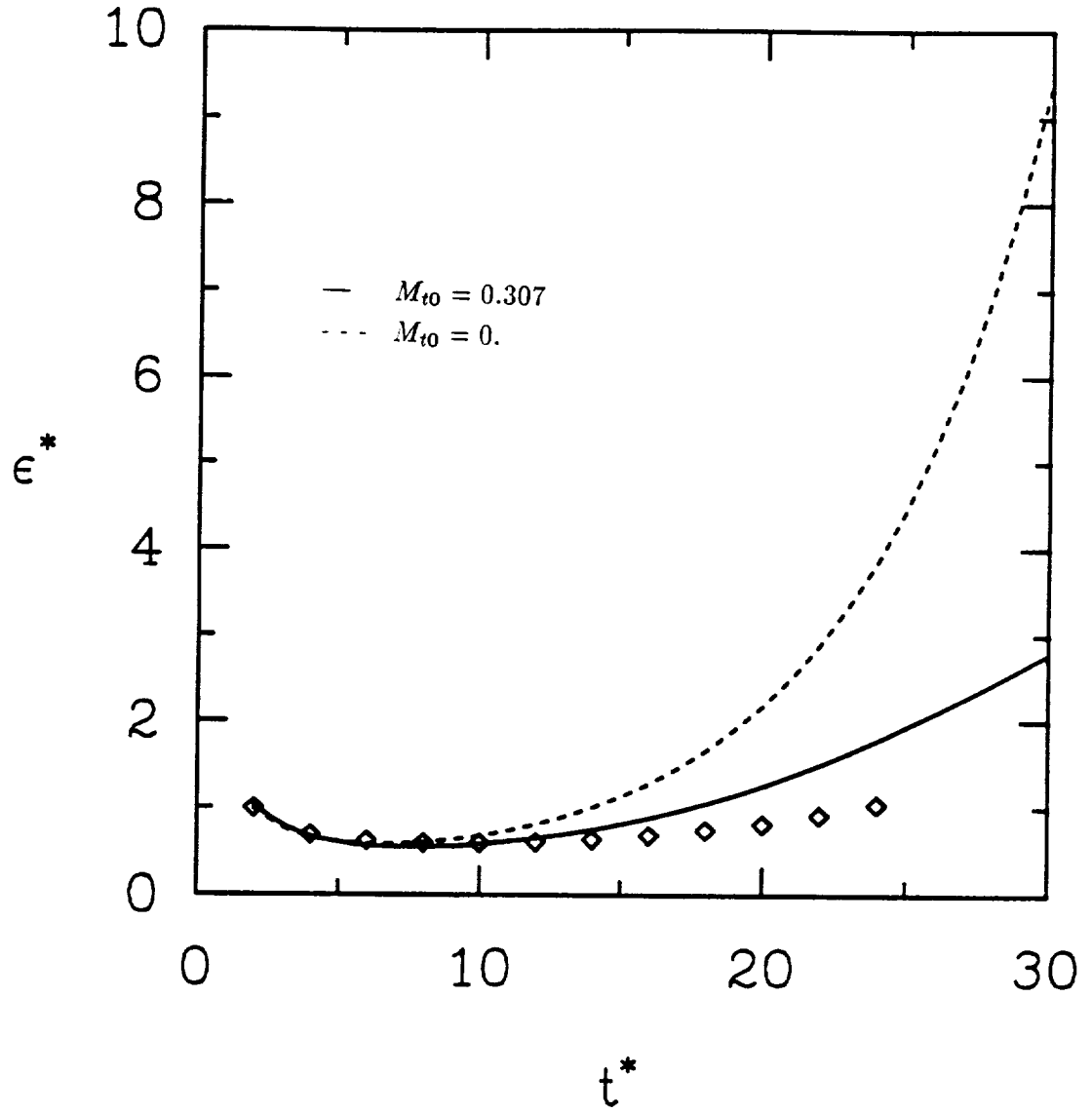


Figure 4. Comparison of the predictions of the SSG model for the time evolution of the total dissipation-rate with the DNS results of Blaisdell.

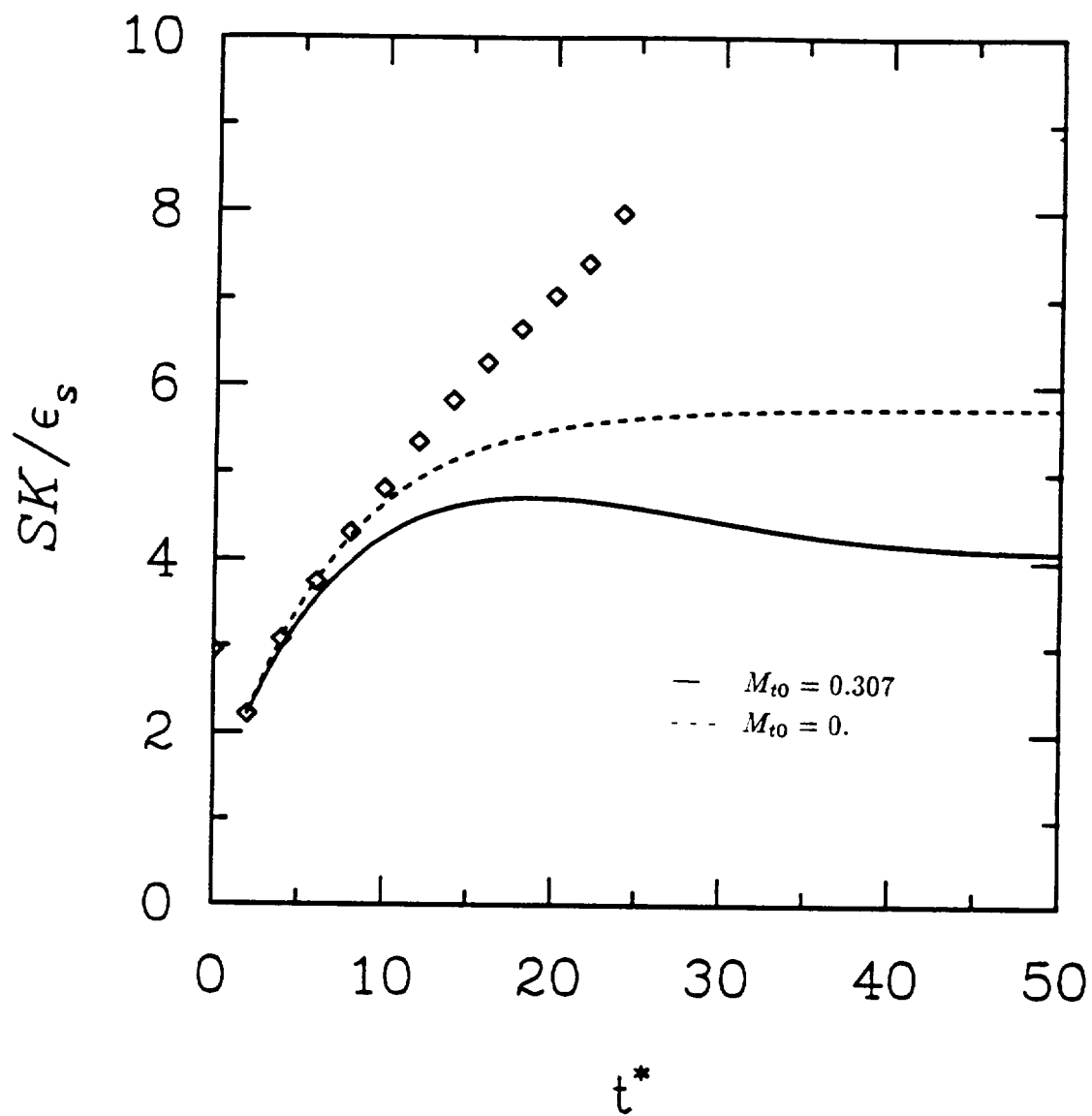


Figure 5. Comparison of the predictions of the SSG model for the time evolution of SK/ϵ_s with the DNS results of Blaisdell.

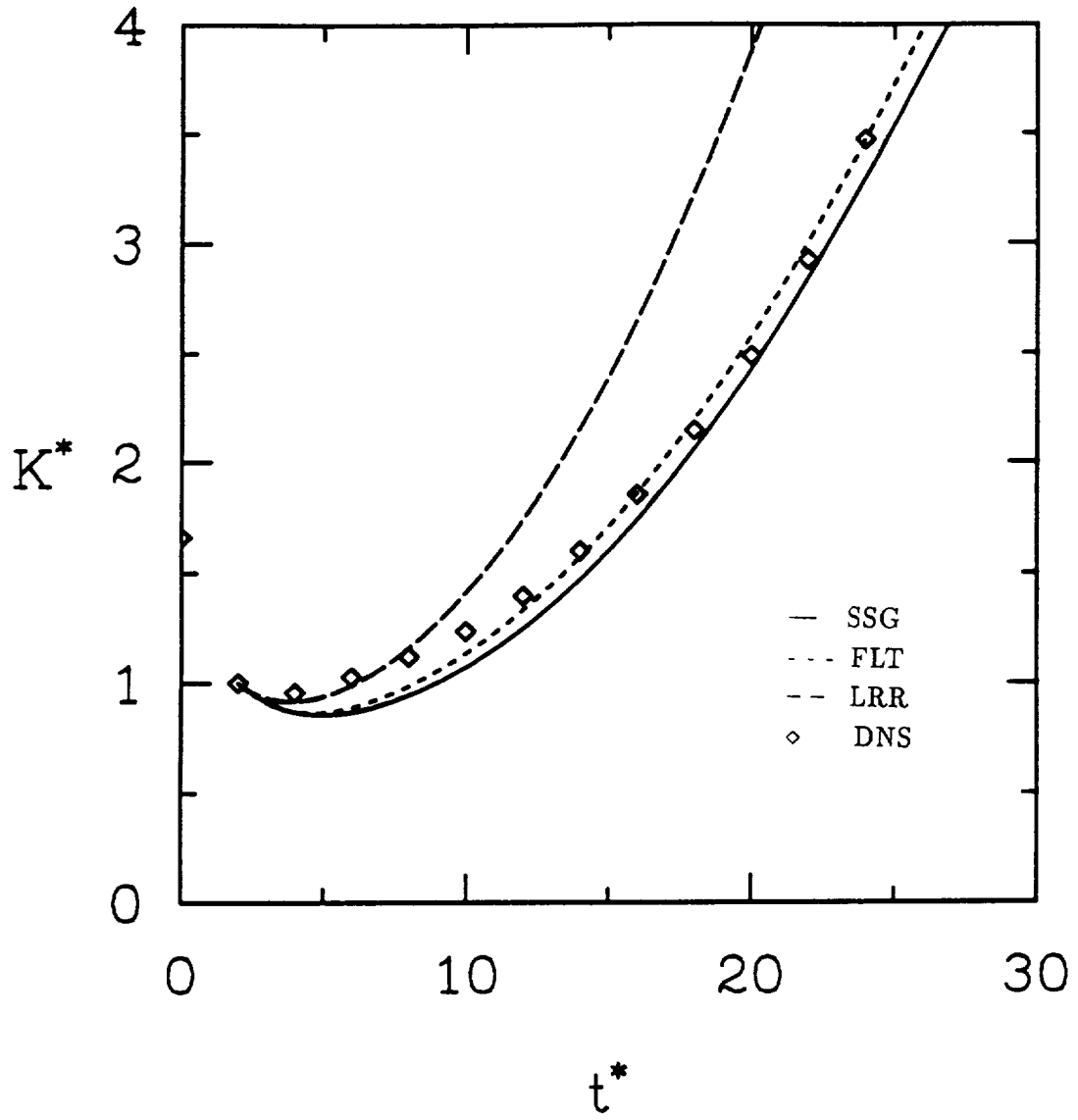


Figure 6. Comparison of the predictions of the LRR, SSG and FLT models for the time evolution of the turbulent kinetic energy with the DNS results of Blaisdell.

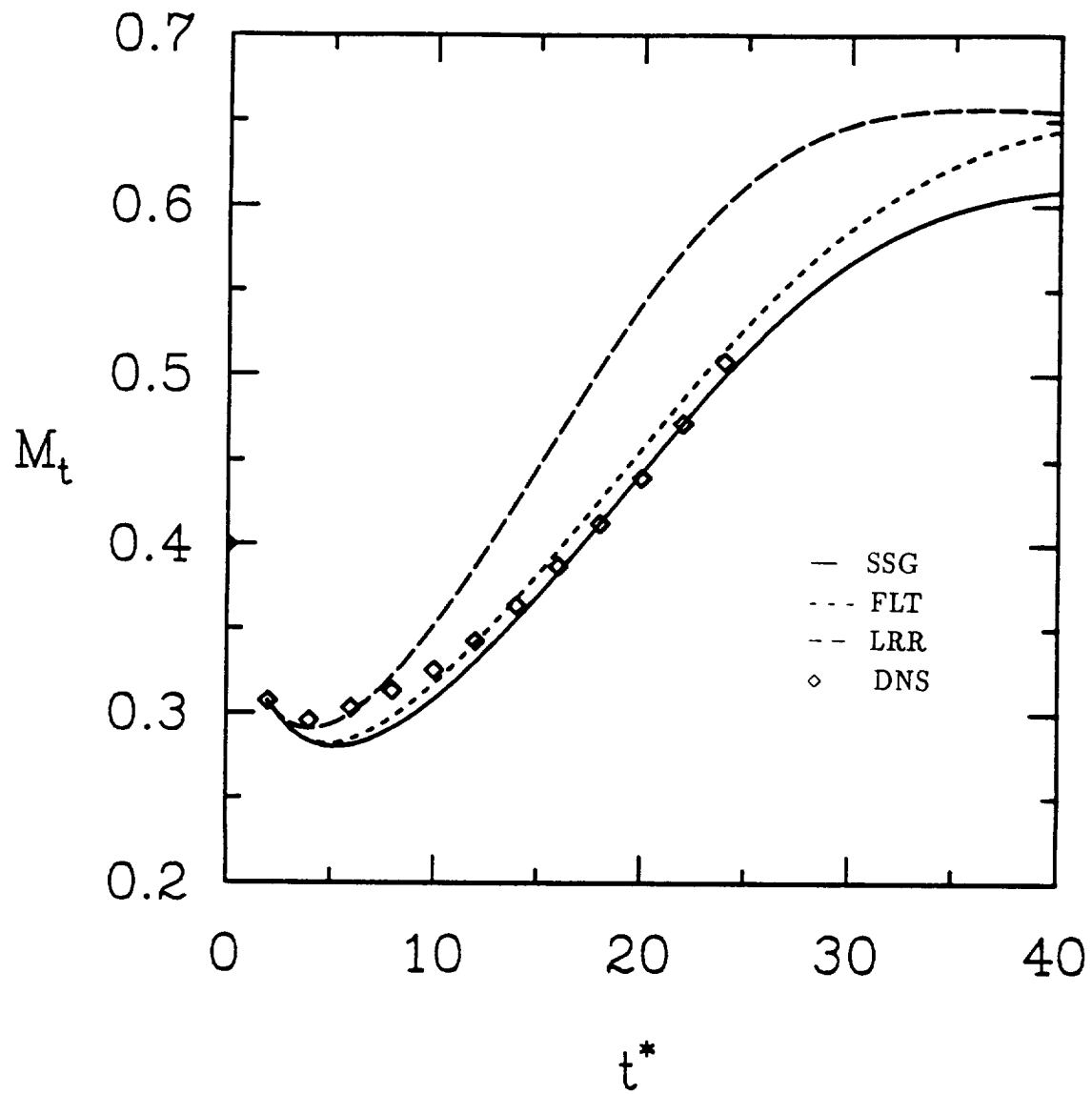


Figure 7. Comparison of the predictions of the LRR, SSG and FLT models for the time evolution of the turbulent Mach number with the DNS results of Blaisdell.

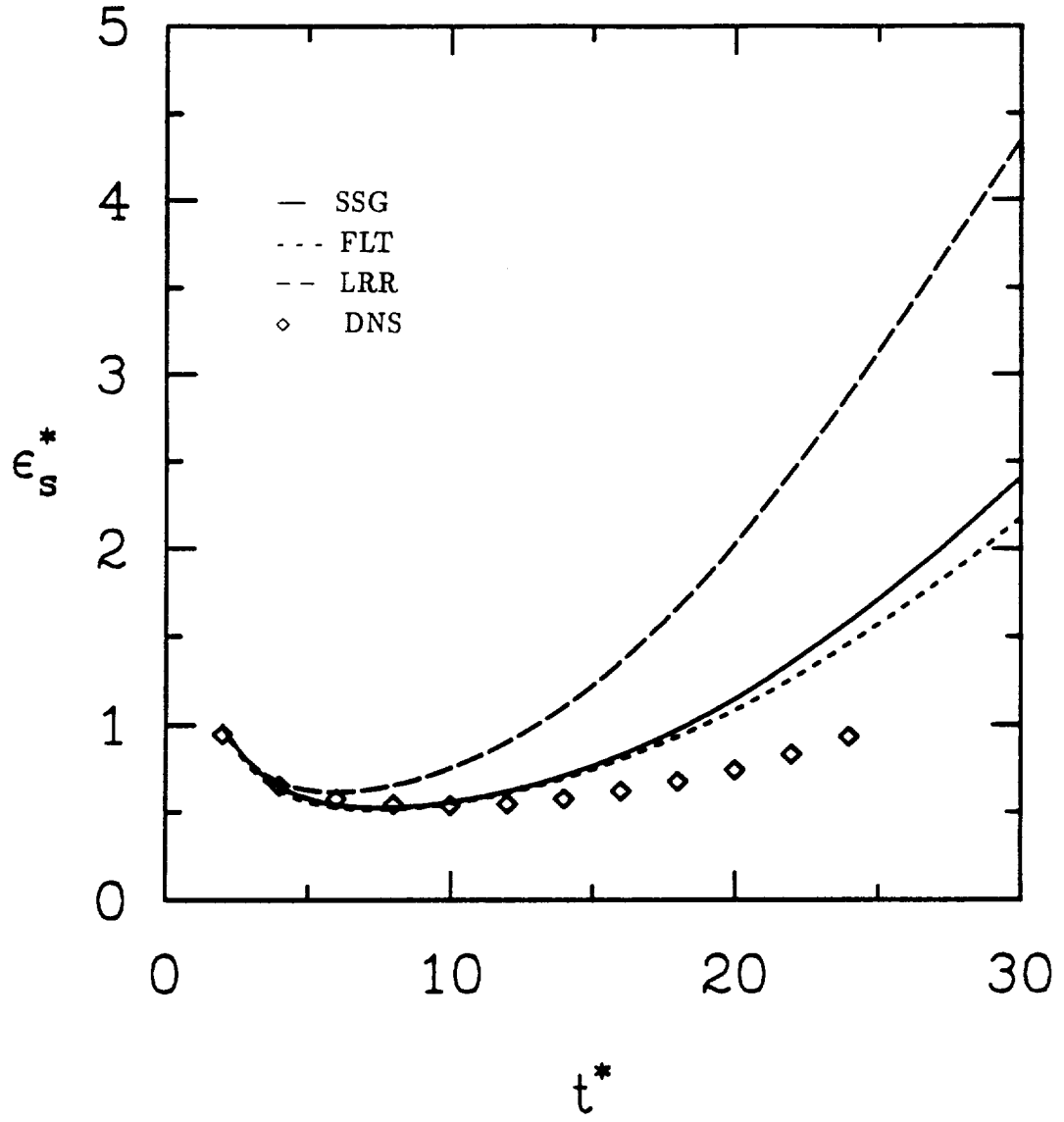


Figure 8. Comparison of the predictions of the LRR, SSG and FLT models for the time evolution of the solenoidal dissipation-rate with the DNS results of Blaisdell.

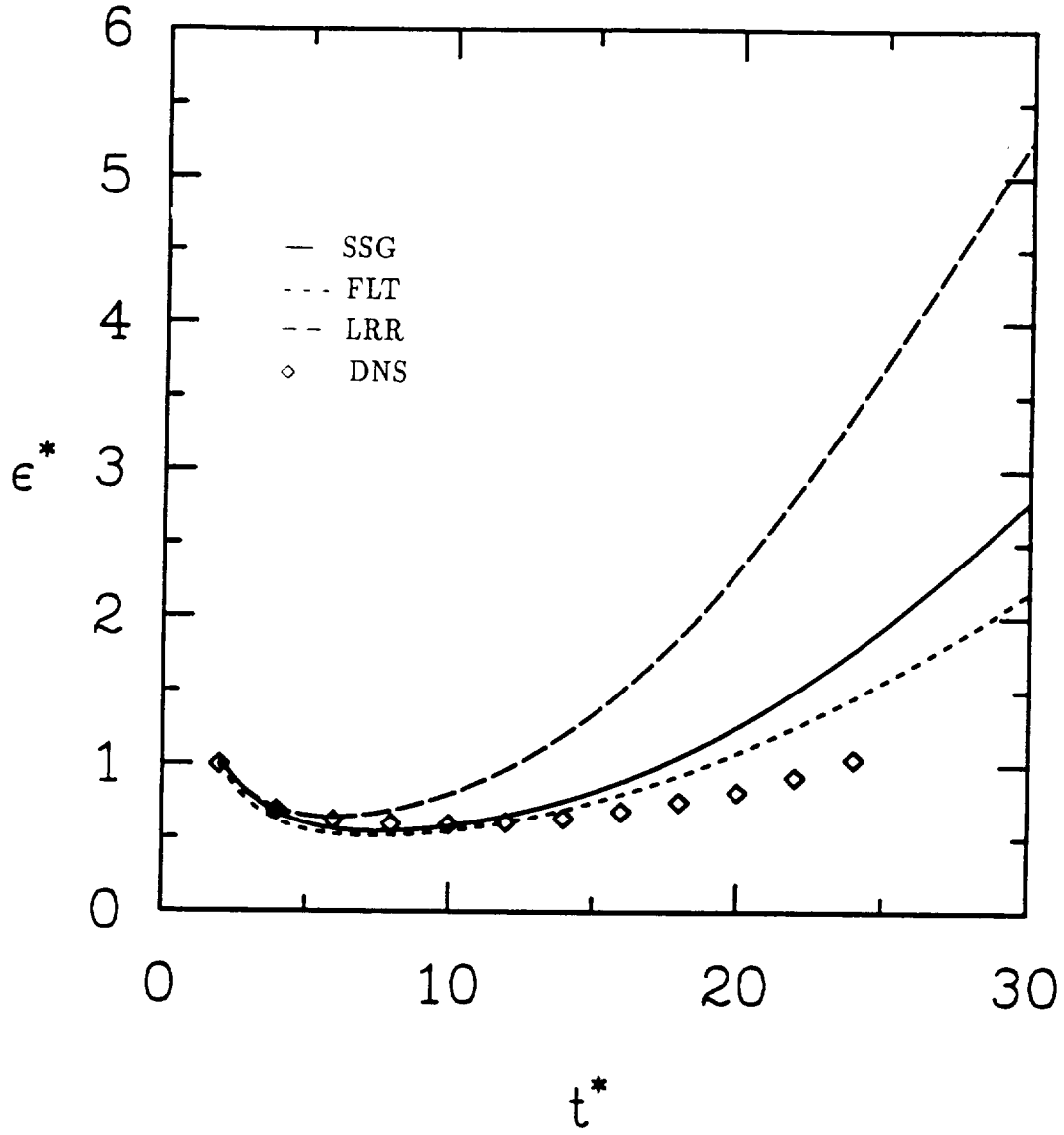


Figure 9. Comparison of the predictions of the LRR, SSG and FLT models for the time evolution of the total dissipation-rate with the DNS results of Blaisdell.

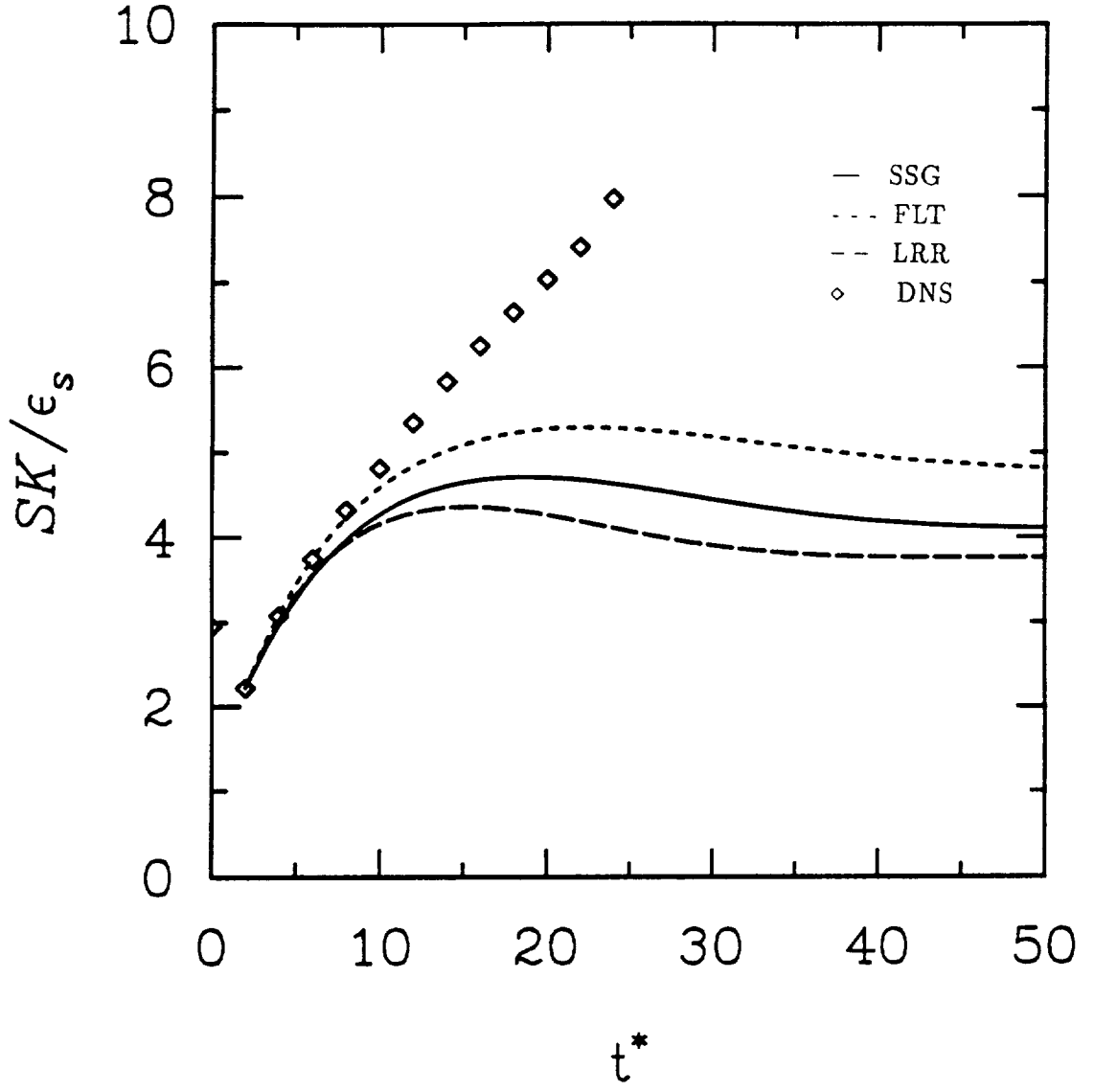


Figure 10. Comparison of the predictions of the LRR, SSG and FTL models for the time evolution of SK/ϵ_s , with the DNS results of Blaisdell.

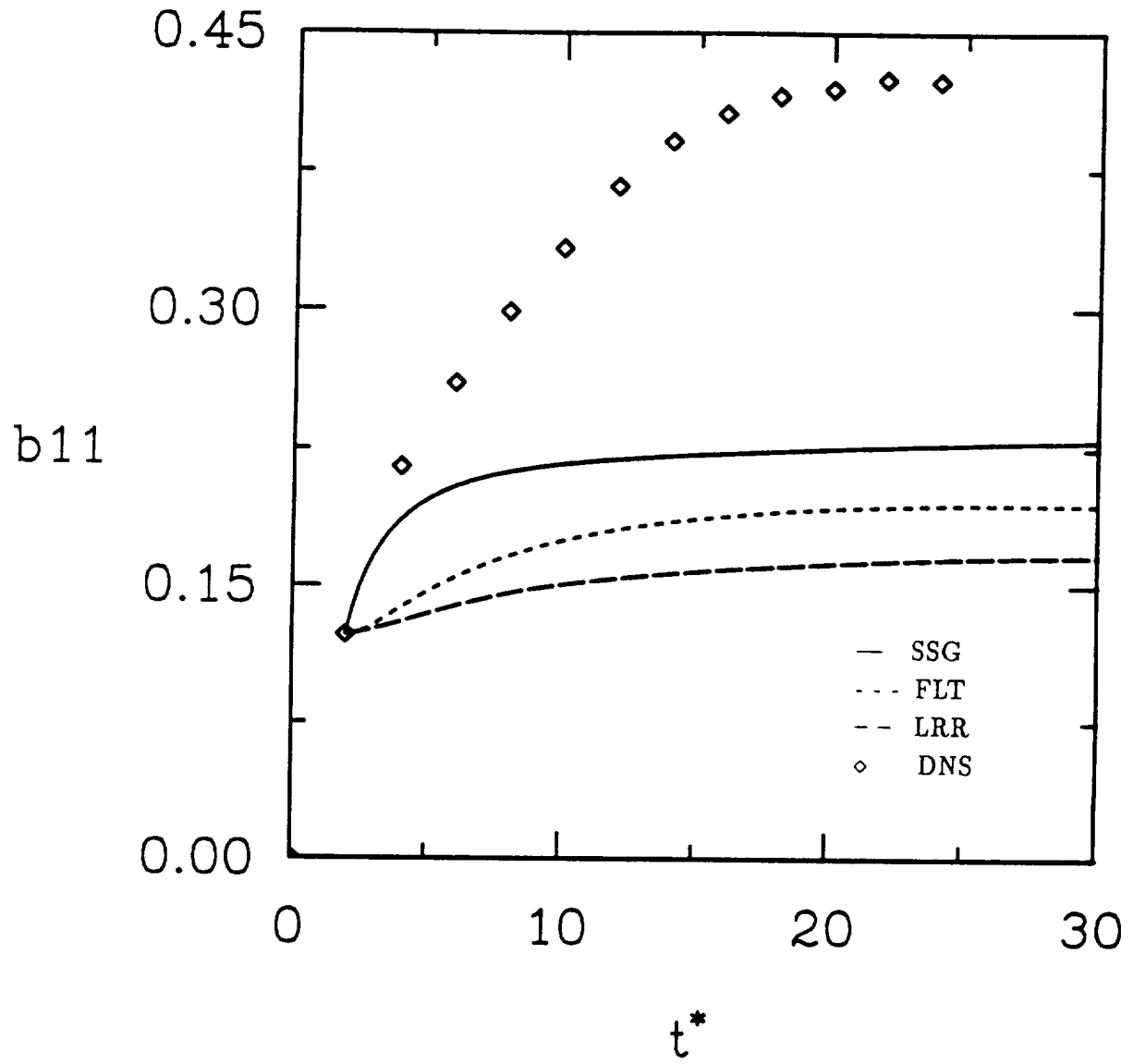


Figure 11. Comparison of the predictions of the LRR, SSG and FLT models for the time evolution of the component b_{11} of the Reynolds stress anisotropy tensor with the DNS results of Blaisdell.

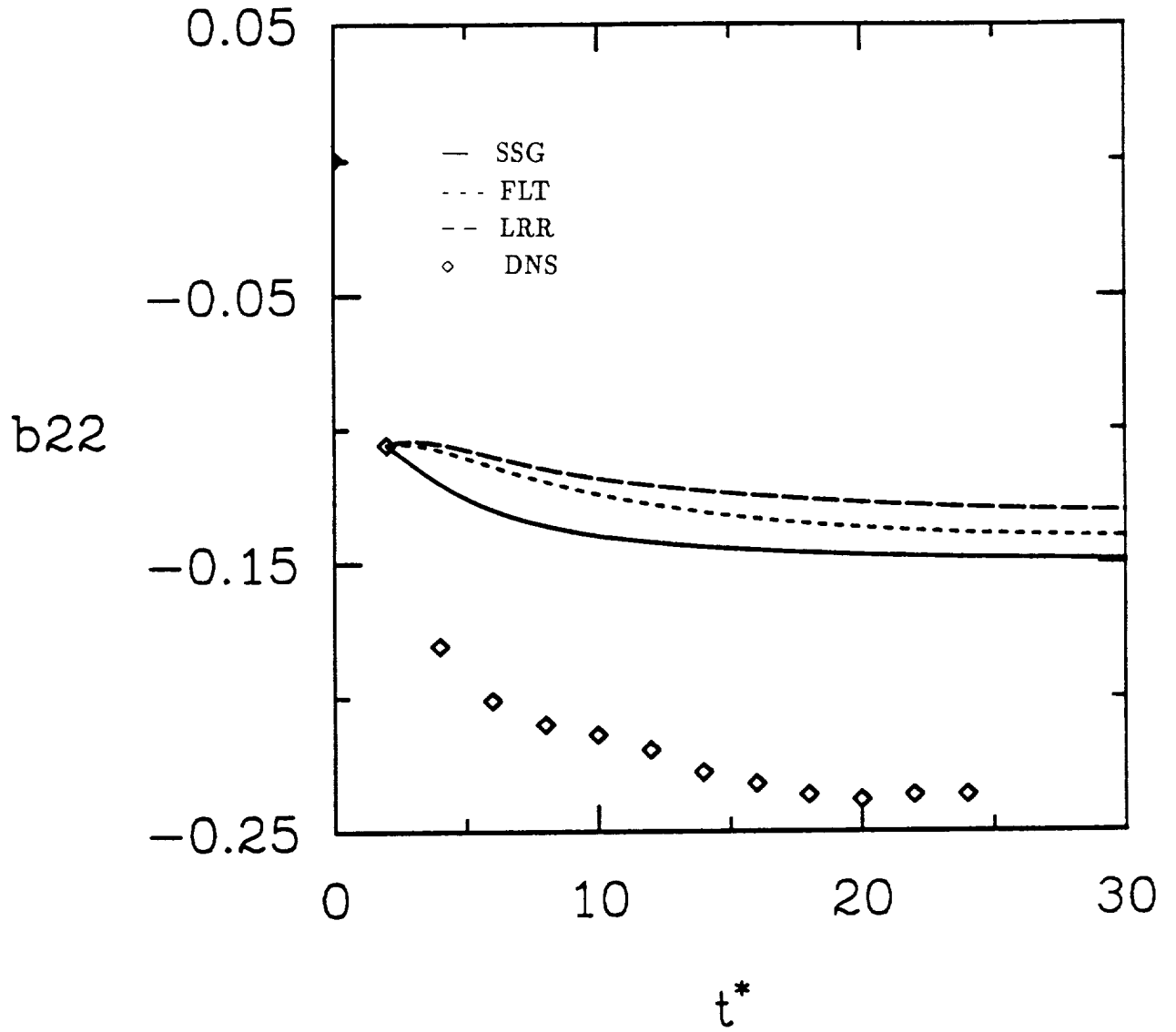


Figure 12. Comparison of the predictions of the LRR, SSG and FLT models for the time evolution of the component b_{22} of the Reynolds stress anisotropy tensor with the DNS results of Blaisdell.

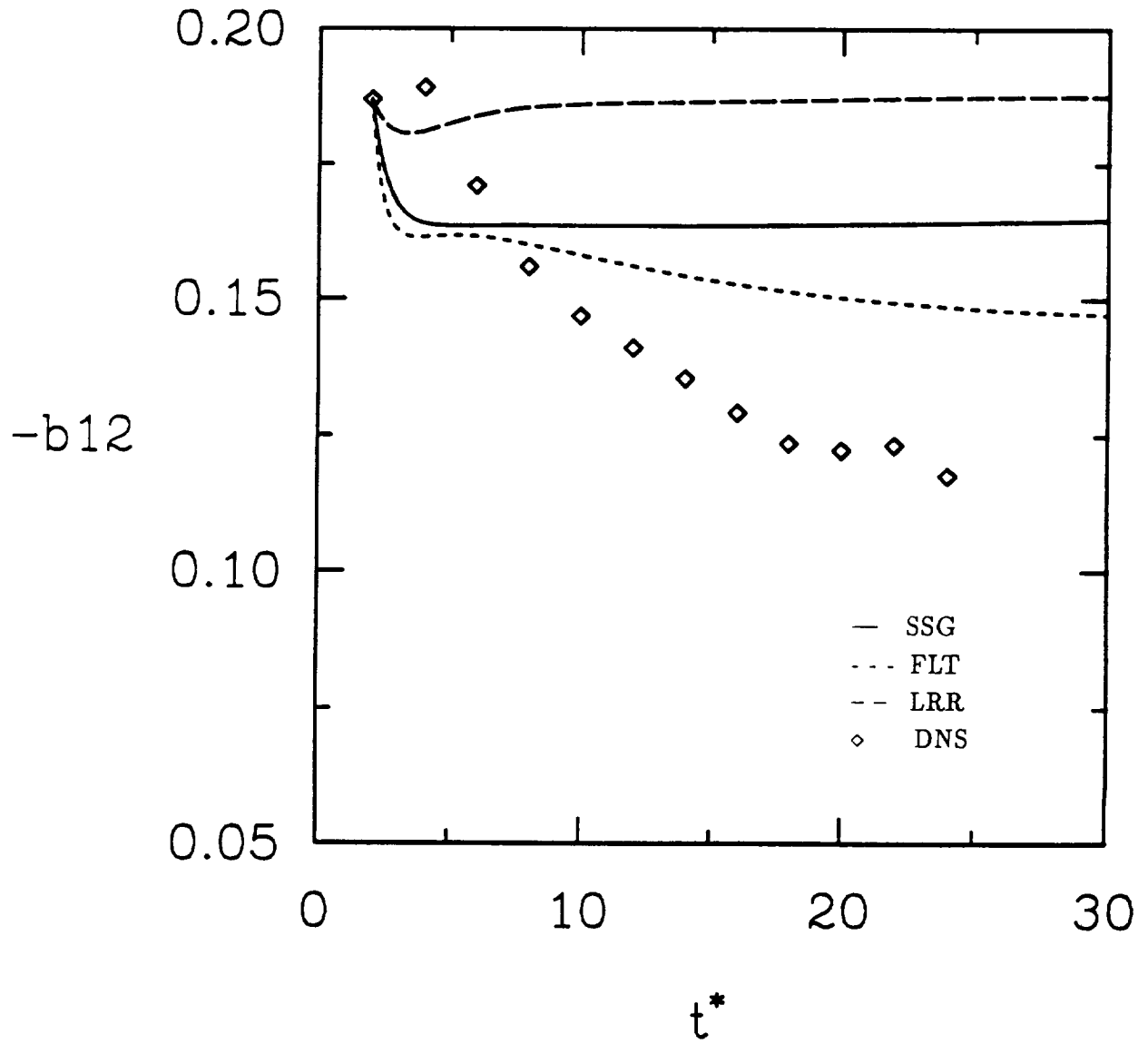


Figure 13. Comparison of the predictions of the LRR, SSG and FLT models for the time evolution of the component b_{12} of the Reynolds stress anisotropy tensor with the DNS results of Blaisdell.

REPORT DOCUMENTATION PAGE			Form Approved OMB No. 0704-0188	
Public reporting burden for this collection of information is estimated to average 1 hour per response, including the time for reviewing instructions, searching existing data sources, gathering and maintaining the data needed, and completing and reviewing the collection of information. Send comments regarding this burden estimate or any other aspect of this collection of information, including suggestions for reducing this burden, to Washington Headquarters Services, Directorate for Information Operations and Reports, 1215 Jefferson Davis Highway, Suite 1204, Arlington, VA 22202-4302, and to the Office of Management and Budget, Paperwork Reduction Project (0704-0188), Washington, DC 20503.				
1. AGENCY USE ONLY (Leave blank)		2. REPORT DATE March 1994		3. REPORT TYPE AND DATES COVERED Contractor Report
4. TITLE AND SUBTITLE On Prediction of Equilibrium States in Homogeneous Compressible Turbulence			5. FUNDING NUMBERS C NAS1-19299 WU 505-70-62-15	
6. AUTHOR(S) Ridha Abid				
7. PERFORMING ORGANIZATION NAME(S) AND ADDRESS(ES) High Technology Corporation 28 Research Drive Hampton, VA 23666-1325			8. PERFORMING ORGANIZATION REPORT NUMBER	
9. SPONSORING / MONITORING AGENCY NAME(S) AND ADDRESS(ES) National Aeronautics and Space Administration Langley Research Center Hampton, VA 23681-0001			10. SPONSORING / MONITORING AGENCY REPORT NUMBER NASA CR-4570	
11. SUPPLEMENTARY NOTES Langley Technical Monitor: Thomas B. Gatski				
12a. DISTRIBUTION / AVAILABILITY STATEMENT Unclassified/Unlimited Subject Category 34			12b. DISTRIBUTION CODE	
13. ABSTRACT (Maximum 200 words) Direct numerical simulations of compressible, homogeneous, turbulent shear flows are used to evaluate Reynolds stress models. Three pressure-strain models, which are either linear, quadratic, or cubic in the anisotropy tensor, are considered. Dilatational dissipation and pressure-strain correlation models do not correctly capture the compressibility effects seen in the direct simulations. In particular, the increase in the anisotropy of normal stresses and the reduction in the shear stress are not reproduced by any of the models. Also, the use of the incompressible form of the dissipation-rate equation to determine the solenoidal part of the dissipation is found to be questionable.				
14. SUBJECT TERMS turbulence, turbulence modeling, compressible flow			15. NUMBER OF PAGES 32	
			16. PRICE CODE A03	
17. SECURITY CLASSIFICATION OF REPORT Unclassified		18. SECURITY CLASSIFICATION OF THIS PAGE Unclassified		19. SECURITY CLASSIFICATION OF ABSTRACT Unclassified
				20. LIMITATION OF ABSTRACT UL

National Aeronautics and
Space Administration
Langley Research Center
Mail Code 180
Hampton, VA 23681-00001

Official Business
Penalty for Private Use, \$300

BULK RATE
POSTAGE & FEES PAID
NASA
Permit No. G-27